 doi:10.20944/preprints202103.0068.v1

Article

Mitigation of Airborne PRRSV Transmission with UV Light Treatment: Proof-of-concept

Peiyang Li[1], Jacek A. Koziel[1]*, Jeffrey J. Zimmerman[2], Jianqiang Zhang[2], Ting-Yu Cheng[2], Wannarat Yim-Im[2], William S. Jenks[3], Myeongseong Lee[1], Baitong Chen[1], Steven J. Hoff[1]

[1] Department of Agricultural and Biosystems Engineering, Iowa State University, Ames, Iowa, USA; peiyangl@iastate.edu (PL); koziel@iastate.edu (JK); leefame@iastate.edu (ML); baitongc@iastate.edu (BC); hoffer@iastate.edu (SH)
[2] Department of Veterinary Diagnostic and Production Animal Medicine, Iowa State University, Ames, Iowa, USA; jjzimm@iastate.edu (JJZ); jqzhang@iastate.edu (JZ); tycheng@iastate.edu (TC); wyimim@iastate.edu (WY);
[3] Department of Chemistry, Iowa State University, Ames, Iowa, USA; wsjenks@iastate.edu (WJ)
* Correspondence: koziel@iastate.edu; Tel.: +1 515-294-4206

Abstract: Proper treatment of infectious air could potentially mitigate the spread of airborne viruses such as porcine reproductive and respiratory syndrome virus (PRRSV). The objective of this research is to test the effectiveness of ultraviolet (UV) in inactivating aerosolized PRRSV, specifically, four UV lamps, UV-A (365 nm, both fluorescent and LED-based), "excimer" UV-C (222 nm), and germicidal UV-C (254 nm), were tested. The two UV-C lamps effectively irradiated fast-moving PRRSV aerosols with short treatment times (<2 s). One-stage and two-stage UV inactivation models estimated the UV doses needed for target percentage (%) reductions on PRRSV titer. UV-C (254 nm) dose needed for 3-log (99.9%) reduction was 0.521 and 0.0943 mJ/cm^2, respectively, based on one-stage and two-stage models. An order of magnitude lower UV-C (222 nm) doses were needed for a 3-log reduction, i.e., 0.0882 and 0.048 mJ/cm^2, based on one-stage and two-stage models, respectively. However, the cost of 222-nm excimer lamps is still economically prohibitive for scaling-up trials. The UV-A (365 nm) lamps could not reduce PRRSV titers for tested doses up to 4.11 mJ/cm^2. Pilot-scale or farm-scale testing of UV-C on PRRSV aerosols simulating barn ventilation rates are recommended based on its effectiveness and reasonable costs comparable to HEPA filtration.

Keywords: air purification, animal production, porcine reproductive and respiratory syndrome, livestock health, livestock biosecurity, swine diseases, ultraviolet light

1. Introduction

Since its initial documentation in the late 1980s [1-2], porcine reproductive and respiratory syndrome (PRRS) has been one of the most impactful diseases affecting the US swine industry. The disease has two overlapping clinical symptoms, reproductive failure or impairment, as well as respiratory diseases. The annual cost of PRRS disease to the producers in the US was estimated to be $560 million estimated in 2005 [3], $664 million in 2012 [4], and $580 million in 2016 [5]. The cost per pig ranged from $6.25 to $15.25 in the market [4][6]. The battle against PRRS is still among the top priorities for producers and veterinarians.

PRRSV can be transmitted via indirect contact (such as aerosol and fomites) or direct contact, but it likewise is found in aerosols generated by infected pigs and reach susceptible pigs, meters or perhaps kilometers away [7-10]. Research suggests that infectious PRRSV aerosols may travel up to ~9 km [11,12]. Given its infectivity and airborne survivability, proper treatment or decontamination of PRRSV aerosols could effectively reduce transmission.

Preprints (www.preprints.org) | NOT PEER-REVIEWED | Posted: 2 March 2021 doi:10.20944/preprints202103.0068.v1

Mitigation against PRRS has been investigated at both laboratory and farm scales, including but not limited to air filtration, air ionization [13], non-thermal plasma (NTP) reactor [14], UV treatment [15], vaccination [16], depopulation [17].

In terms of air filtration, high-filtration efficiency air filters (MERV, HEPA) have been used by selected swine operations to treat incoming ventilation air and prevent barns from infectious airborne viruses. These filters were proven to effectively prevent the transmission of PRRSV [18,19]. However, maintenance of these filters is labor-intensive and requires expensive addition to barn space. Thus, very few facilities in the US can afford mechanical filtration of incoming air. A more affordable way of defending swine barns from incoming infectious air is needed for industry.

Ultraviolet (UV) light, especially ultraviolet-C (UV-C, ranging from 200 – 280 nm), has been proven to disinfect or inactivate pathogens. In theory, UV can potentially reduce operational and capital costs by eliminating the requirement for high-grade filters. To date, very little research has been published on the use of UV for aerosolized PPRSV inactivation. At present, Cutler et al. (2012) [20] remains the benchmark study on UV-C treatment of aerosolized PRRSV. UV-C (254 nm) inactivation and parameters under static conditions (i.e., no aerosol generation) were reported by Cutler et al. (2011) [21] for both one-stage and two-stage models. Under dynamic conditions (i.e., irradiation on PRRSV aerosols), only a one-stage model was reported by [20]. The estimations on UV-C (254 nm) dose needed to inactivate practical PRRSV levels (e.g., 90%, 99%, 99.9%) remain very limited. In addition, the routine use of UV 254 nm on farms raises concerns about its potentially harmful effects on both workers and animals.

More recently, reports on the inactivation of pathogens using 'excimer' UV-C *in vitro* have appeared [22-23]. The excimer lamp (207 – 222 nm in the UV-C range) poses less risk to humans (innocuous to mammalian skins and eyes) compared with 254 nm, while still being germicidal for Methicillin-resistant *Staphylococcus aureus* (MRSA) [22] and H1N1 influenza virus [23]. There is no published data on the effectiveness of UV-C excimer (207 – 222 nm) to treat airborne PRRSV. Similarly, there is no published data on the inactivation of aerosolized PRRSV using UV-A (315 - 400 nm). UV-A is commonly known as 'black-light', considered less toxic, and used for, e.g., artificial sun tanning. Recent research has shown that both UV-C and UV-A can be effective in mitigating emissions of odor, odorous volatile organic compounds (VOCs), a potent greenhouse gas (N_2O), ammonia (NH_3) [24-29] on lab- and pilot-scales. Thus, there is an opportunity to consider that UV treatment could be beneficial to mitigate *both* gaseous emissions and the pathogen load.

Given this background, we addressed specific objectives in this laboratory-scale proof-of-concept research:

Obj. 1. Quantify and compare the inactivation of aerosolized PRRSV by UV-C germicidal (254 nm), UV-C 'excimer' (222 nm), UV-A fluorescent (365 nm), and UV-A LED (365 nm).

Obj. 2. Estimate the UV-A and UV-C dose needed for 90%, 99%, and 99.9% reduction in infectious aerosolized PRRSV.

Obj. 3. Evaluate the techno-economic feasibility of UV treatment for airborne PRRSV in a swine barn inlet air.

This research is a subsequent study following Li et al. (2021) [30] and Koziel et al. (2020) [31], where a system of PRRSV aerosolization, sampling, and recovery was designed, built, and verified.

2. Materials and Methods

2.1. Experiment Overview (Obj. 1)

The experimental setup (Figure 1) consisted of three major sections: (i) aerosolization section, (ii) treatment section, and (iii) sampling section, in the order of the airflow direction. Section (i) provided for PRRSV aerosolization, airflow regulation, and monitoring; Section (ii) provided the PRRSV aerosol-controlled UV exposure; Section (iii) sampled the aerosolized PRRSV after UV-treatment. The impinger solution was tested for viable

Preprints (www.preprints.org) | NOT PEER-REVIEWED | Posted: 2 March 2021 doi:10.20944/preprints202103.0068.v1

PRRSV, and the concentration was expressed as median tissue culture infectious dose ($TCID_{50}$).

The setup and procedure were based on Li et al. (2021) [30], except Section (ii), treatment section, was installed with UV lamps to irradiate fast-moving PRRSV aerosols.

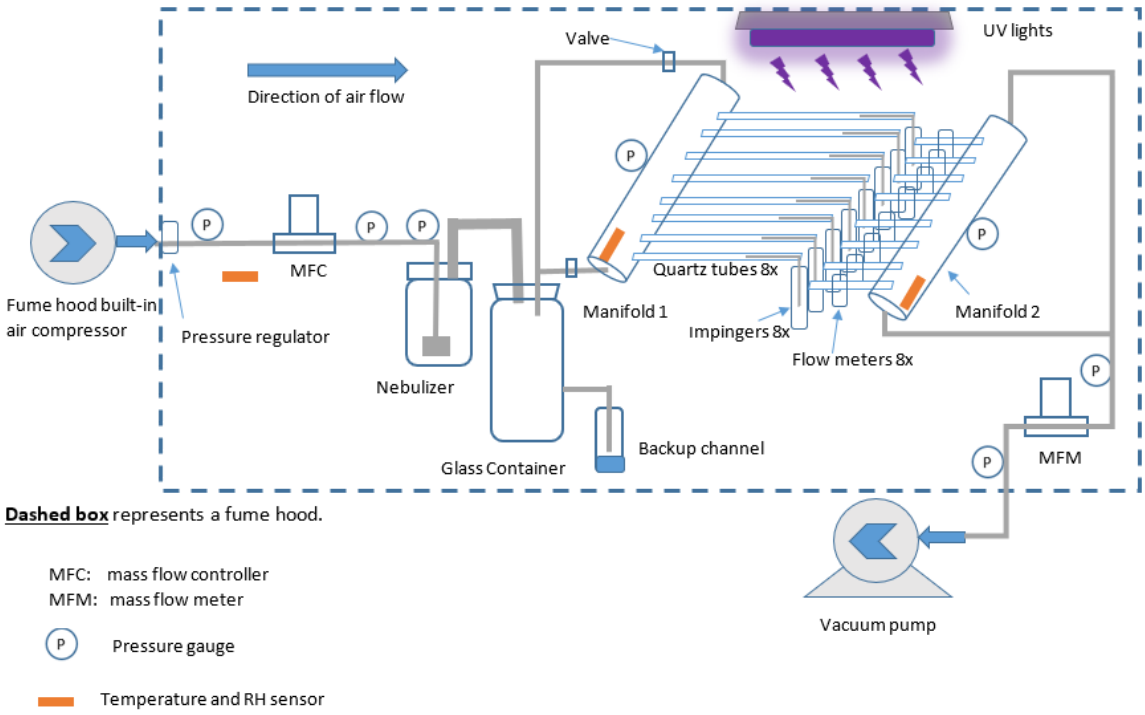

Figure 1. Experimental setup for PRRSV aerosol generation, UV treatment, and collection of treated PRRSV aerosols inside a fume hood.

Experimental procedures, e.g., PRRSV aerosolization and aerosol sampling, were conducted in a BSL-1 setting (3214 Sukup Hall, Iowa State University), and the virus isolation was conducted in a BSL-2 laboratory (Veterinary Diagnostic Laboratory, College of Veterinary Medicine, Iowa State University).

2.2. PRRSV Propagation and Aerosolization (Preparation for Obj .1)

The PRRSV used in this experiment (MN-184, PRRSV-2 Lineage 1) was provided by the Veterinary Diagnostic Laboratory (College of Veterinary Medicine, Iowa State University). The virus was propagated in the MARC-145 cell line, a clone of the African monkey kidney cell line MA-104 (Kim et al. 1993) [32]. The details of PRRSV propagation and storage are fully described in [24]. The propagated virus inoculum had a virus titer of $1 \times 10^{5.56}$ $TCID_{50}$/mL.

To generate PRRSV aerosols, compressed air first passed through a mass flow controller (MFC) (model#: GFCS-010013, Aalborg Instruments & Controls Inc., Orangeburg, New York, USA) and then to a 24-jet Collison nebulizer (formerly BGI Inc., now CH Technologies, Westwood, NJ, USA) [30]. The nebulizer was prefilled with 60 mL of PRRSV inoculum with 0.2% (v/v) antifoam A emulsion (Sigma-Aldrich Corp., St. Louis, MO, USA) and 2 ppm of Rhodamine B powder (Sigma-Aldrich Corp., St. Louis, MO, USA). Antifoam A was previously shown to reduce foaming, with no harmful effect on laboratory cultured cells or PRRSV itself [33]. The nebulizer aerosolized ~35 mL of PRRSV inoculum under a pressure of around 20 psi in each (~45-min) experiment. PRRSV aerosols were directed to the glass container (3 gals, or 12 L) and then into Manifold 1, where they were distributed into eight branches (quartz tubes) for UV irradiation.

2.3. UV light selections and measurements (Obj. 1)

Preprints (www.preprints.org) | NOT PEER-REVIEWED | Posted: 2 March 2021 doi:10.20944/preprints202103.0068.v1

2.3.1 UV light selections

Four types of UV light with three different wavelengths were used: i) 365-nm UV-A fluorescent black light blue (BLB) light (F15T8BLB) (Ushio America Inc., Cypress, CA, USA), ii) 365-nm UV-A LED lights (research-grade prototype, LED board + power supply) (Once Inc., Plymouth, MN, USA), iii) 222-nm UV-C excimer light (Ushio America Inc., Cypress, CA, USA), and iv) 254-nm UV-C germicidal light (G15T8) (Ushio America Inc., Cypress, CA, USA).

The UV-A fluorescent (365 nm) and UV-C germicidal (254 nm) bulbs were mounted in two XX-15A UV fixtures, respectively (Spectronics Corp., New York, NY, USA). Each fixture could accommodate two lamps, with each consuming 15 watts of power, although the full UV power is just a fraction of it. The LED lamp for UV-A (365 nm) was a square-shaped plate (0.3 x 0.3 m; 1 x 1 ft) mounted with dozens of small LED bulbs, equipped with an additional power supply. The UV-C excimer (222 nm) lamp was a single-bulb system with a customized power supply and its nominal power consumption of 300 W.

2.3.2 UV light intensity measurement

The light intensity was measured (ILT 1700 radiometer, International Light Technologies, Peabody, MA, USA) using wavelength-specific sensors and filters. Four combinations of sensor/probe were used for the measurement of each lamp: i) SED240 sensor added with an NS254 filter that can measure a center wavelength of 254 nm, with a tolerance range of 254~257 nm; ii) SED240 sensor equipped with an NS220 filter that can measure a center wavelength of 220 nm, with a tolerance range of 219~223 nm; iii) SED033 sensor with an NS365 filter that has a tolerance range of 365~367 nm (manufacturer information). The radiometer, all detectors, and filters were factory-calibrated before measurements. All UV lamps were turned on for 5 min before each measurement to ensure steady, stable, and consistent irradiation. During the light intensity measurements, the radiometer sensors were positioned 10 cm directly underneath the UV lights.

To better understand the UV intensity inside the quartz tube, the tubes were horizontally cut in half to allow the sensor to be positioned directly underneath the top half. The UV light intensity measurement was conducted on the layout of eight quartz tubes. Quartz tubes were used in this experiment as channels to carry and separate PRRSV aerosols. The circular, cross-sectional area of the tubes created difficulty when measuring and estimating UV light intensity and dose, as the UV sensor probe cannot be inserted inside for the real measurement. Therefore, we cut the quartz tube horizontally in half when measuring the light intensity. Seven equally spaced (~4 cm) points were measured over the length of each tube. In total, the light intensity at 56 points was measured, and an irradiation map was drawn for each type of UV. Figures B1-B4 in Appendix B show the maps of UV light intensity (irradiation) for all four types of UV lamps used in this experiment. Supplementary Figures S1 – S5 present the UV lamps used in this experiment and an example of light intensity measurement.

During each experiment, the UV sensor was positioned at a reference point near Manifold 1 for monitoring purposes to ensure that the lamps were functioning normally. The summary of UV light intensity data was recorded in Table 1 (details included in Supplementary Tables 1 – 4).

Table 1. Average UV light intensity for each treatment (quartz tube #) measured without tube shielding. In the experiment, the quartz tubes were covered with different lengths of PVC pipes to control the UV dose, and thus the effective light intensity was estimated for each treatment separately.

	UV light intensity (mW/cm²)			
	UV-C (254 nm)	**UV-C (222 nm)**	**UV-A (365 nm, fluorescent)**	**UV-A (365 nm, LED)**
Treatment 1*	0.11	0.028	0.57	1.71

Preprints (www.preprints.org) | NOT PEER-REVIEWED | Posted: 2 March 2021 doi:10.20944/preprints202103.0068.v1

Treatment 2	0.14	0.039	0.70	1.93
Treatment 3	0.15	0.041	0.77	2.00
Treatment 4	0.16	0.044	0.80	2.02
Treatment 5	0.16	0.042	0.79	2.01
Treatment 6	0.15	0.043	0.74	1.99
Treatment 7	0.13	0.042	0.66	1.90
Treatment 8	0.10	0.039	0.49	1.66

*Treatment 1 refers to quartz tube 1. The same rule applies to all the treatments.

2.4 *UV treatment of aerosolized PRRSV*

Eight identical quartz tubes (ID = 25 mm, OD = 28 mm, length = 30 cm) (Technical Glass Products Inc., Painesville Twp., OH, USA) were positioned horizontally with an equal gap (5 cm) between each. Both ends of each tube were connected with plastic tubes and sealed by parafilm. The UV lights were placed on top of the tubes, 10 cm from the tubes' central horizontal plane. Also, note that the lamps were positioned horizontally at 90 degrees to the quartz tubes. This setting was intended to create a more uniform distribution of UV across the eight tubes.

Each treatment (quartz tube) represented a different level of UV dose. This was achieved by shielding different lengths of the quartz tubes with PVC tubes that were tailored to cover a desired section of the quartz, thereby achieving various treatment (UV exposure) times. The shielding options were: 14.3%, 28.6%, 42.9%, 57.2%, 71.5%, 85.8%, 100.1% of the length of each quartz tube. The treatment times (calculated by dividing the exposed tube length by aerosol velocity) were 1.81 s, 1.55 s, 1.29 s, 1.03 s, 0.77 s, 0.52 s, 0.26 s, 0 s, i.e., from exposed to fully shielded. The layout of the treatments is shown in Figure B5 in Appendix B and the illustrative photo is shown in Figure S6. For each type of UV, four (n=4 replications) experiments were conducted.

The Bunsen-Roscoe Reciprocity Law dictates the calculation of the UV dose:

$$D = I \times T \quad (1)$$

Where D is the UV dose (mJ/cm^2), I is irradiance or light intensity (mW/cm^2), and T is the UV treatment time (s).

2.5 *Post-UV-irradiation aerosol collection, recovery, and PRRSV titer calculation (Obj. 1)*

Before each experiment, the UV light was turned on for 5 min to stabilize UV irradiation. After that, the vacuum pump was turned on, immediately followed by opening the compressed air valve. The rear (right side) end of each quartz tube was connected to a glass AGI 7541 impinger (Ace Glass Inc., Vineland, NJ, USA) with a flow rate of 6 L/min. Each impinger was filled with 15 mL of PBS and 0.1% (v/v) antifoam A emulsion. The impingers function by impacting aerosolized virus onto the surface of the liquid. Thereafter, the liquid was tested to determine its concentration of infectious virus. Downstream of each impinger was a flow meter (Catalog No. RMA-21-SSV, Dwyer Instruments Inc., Michigan City, IN) to adjust the flow rate to achieve equal distribution of the flow across the tubes. The sample collection time was 45 min per experiment. Desiccation of impinger fluid is sometimes a problem in aerosol collection experiments. In this study, minimal impinger fluid loss was noted, i.e., < 2 mL.

To determine the infectious virus titer, impinger fluid was transferred to a biosafety cabinet in a BSL-2 laboratory for 10-fold serial dilutions performed on 96-well plates, with eight replicates for each sample. Each well in 96-well plates (except for the first row) was prefilled with 270 µL of RPMI-1640 medium, and then the sample was added to the plates' first row. The solution was then mixed, and 30 µL of liquid was transferred sequentially from one row to another. Thus, the dilution for each row ranged from 10^0, 10^{-1}, …, to 10^{-7}, respectively. Thereafter, 100 µL from each well was inoculated into subconfluent MARC-145 cells grown in 96-well plates. The plates were incubated at 37 °C in a humidified 5%

Preprints (www.preprints.org) | NOT PEER-REVIEWED | Posted: 2 March 2021 doi:10.20944/preprints202103.0068.v1

CO_2 incubator. Cytopathic effect (CPE) development was checked under an optic microscope daily, and infected wells were marked as positive until no additional wells were identified as infected (5 to 7 days). To confirm the presence of PRRSV, the cell plates were fixed (80% acetone for 10 min), dried, and then stained with a PRRSV nucleocapsid protein-specific monoclonal antibody (SDOW17-F) conjugated to fluorescent isothiocyanate (Rural Technologies, Inc., Brookings, SD) for 1 h at 37 °C in the incubator. The antibody conjugate was decanted, and the cell plates were washed with PBS (1x pH 7.4) 3 times, 5 min each time. Plates were read under an Olympus IX71 fluorescent microscope (Olympus America Inc., Center Valley, PA, USA) [33]. The Spearman-Kärber method [34-36] was used to calculate the virus titers based on the number of wells showing positive PRRSV-specific fluorescence at specific dilution, and the results were expressed as $TCID_{50}$/mL of the impinger sampling fluid.

2.6 UV inactivation models (Obj. 2)

The statistical analysis was conducted using the *R* statistical program (version 3.6.3, R Studio, Boston, MA, USA). The inactivation models shown in the Results section were based on the one-stage and two-stage microbial survival models mentioned in Kowalski (2000) [37] and Riley et al. (1972) [38]. Briefly, the one-stage microbial inactivation (or reduction) model treated the microbial population as a homogeneous population in which all members are equally susceptible to inactivation, i.e., a monomolecular reaction [37]. In contrast, two-stage inactivation assumes the microbial population is composed of two types, one type more susceptible to UV and one less so. Cutler et al. (2011) [21] analyzed the fitness of one-stage and two-stage inactivation models for static PRRSV inoculum. In this research, the data were processed in both one and two-stage inactivation models.

The one-stage model (adopted from Chick's law),

$$log_{10}N_t = log_{10}N_0 - kD_t + C_1 \quad (2)$$

Rearrange Eqn. [2] to get the fraction of surviving pathogens (log_{10} normalized),

$$log_{10}\frac{N_t}{N_0} = -kD_t + C_1 \quad (3)$$

Where N_t = virus titer ($TCID_{50}$/mL) in the impinger fluid after UV treatment with a D_t
N_0 = virus titer ($TCID_{50}$/mL) in the control sample (without UV exposure)
k = inactivation rate (constant)
D_t = UV dose (mW/cm²), calculated by Eqn. (1)
C_1 = intercept for the one-stage model.

The two-stage model can be expressed as,

$$log_{10}N_t = log_{10}N_0 + log_{10}[(1-f)\cdot 10^{-k_1\cdot D_t} + f\cdot 10^{-k_2\cdot D_t}] + C_2 \quad (4)$$

Rearrange Eqn. [4] to get the fraction of surviving pathogens (log_{10} normalized),

$$log_{10}\frac{N_t}{N_0} = log_{10}[(1-f)\cdot 10^{-k_1\cdot D_t} + f\cdot 10^{-k_2\cdot D_t}] + C_2 \quad (5)$$

1-f = the fraction of the virus population that is more susceptible to UV treatment with an inactivation rate k_1
f = the fraction of the virus population that is more resistant to UV treatment with an inactivation rate k_2
k_1 = inactivation rate for the susceptible fraction of the virus population under UV treatment
k_2 = inactivation rate for the resistant fraction of the virus population under UV treatment
C_2 = intercept for the two-stage model.

3. Results

3.1 Effectiveness of UV to treat airborne PRRSV (Obj. 1)

Preprints (www.preprints.org) | NOT PEER-REVIEWED | Posted: 2 March 2021 doi:10.20944/preprints202103.0068.v1

Figures 2 to 5 summarize the UV inactivation of aerosolized PRRSV. Two curves (one-stage and two-stage) were drawn to show the data fit in the inactivation models.

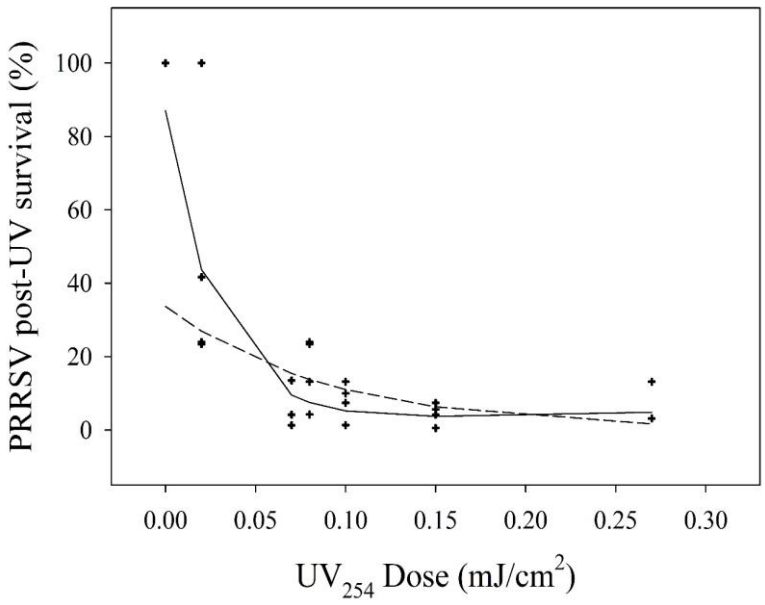

Figure 2. UV-C (254 nm) treatment inactivation of aerosolized PRRSV. PRRSV post-UV survival (%) = Nt/N0. A log10 normalized PRRSV post-UV survival is shown in Figure A1. One-stage and two-stage inactivation models are marked with dashed and solid lines, respectively.

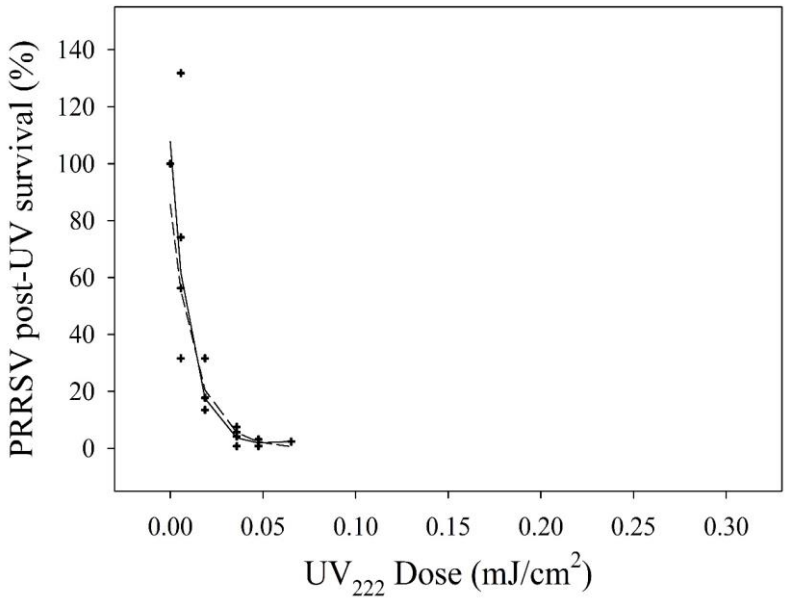

Figure 3. UV-C (222 nm) treatment inactivation of aerosolized PRRSV. PRRSV post-UV survival (%) = N_t/N_0. A $\log_{10}$ normalized PRRSV post-UV survival is shown in Figure A2. One-stage and two-stage inactivation models are marked with dashed and solid lines, respectively.

Preprints (www.preprints.org) | NOT PEER-REVIEWED | Posted: 2 March 2021 doi:10.20944/preprints202103.0068.v1

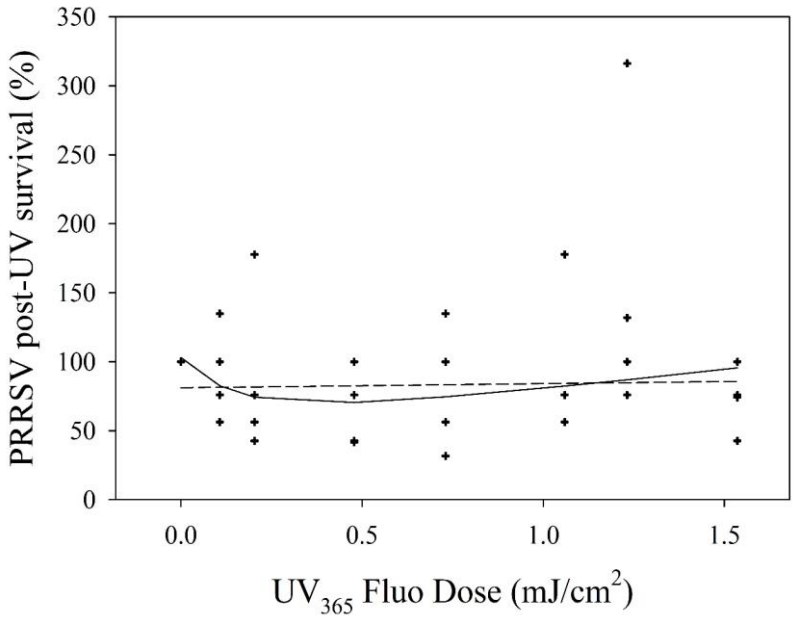

Figure 4. UV-A (365 nm, fluorescent) treatment inactivation of aerosolized PRRSV. PRRSV post-UV survival (%) = N_t/N_0. A $\log_{10}$ normalized PRRSV post-UV survival is shown in Figure A3. One-stage and two-stage inactivation models are marked with dashed and solid lines, respectively.

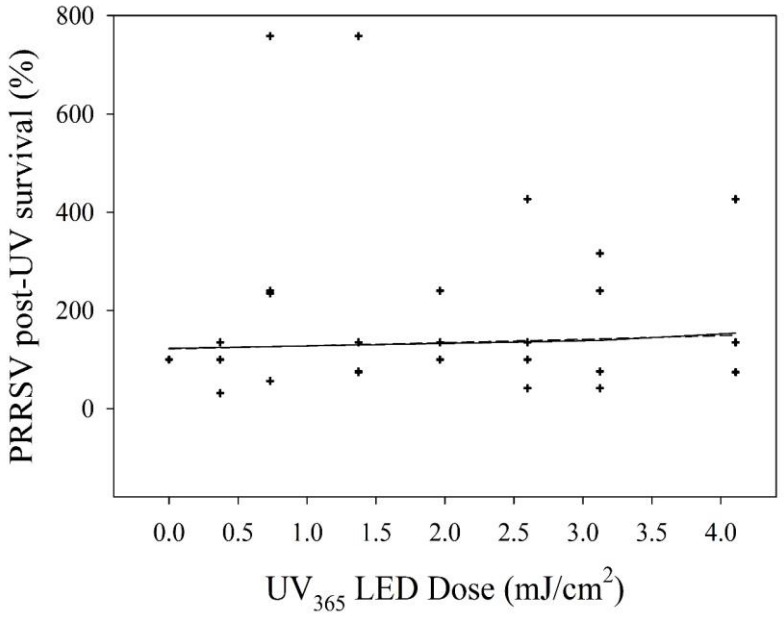

Figure 5. UV-A (365 nm, LED) treatment inactivation of aerosolized PRRSV. PRRSV post-UV survival (%) = N_t/N_0. A $\log_{1supp0}$ normalized PRRSV post-UV survival is shown in Figure A4. One-stage and two-stage inactivation models are marked with dashed and solid lines, respectively.

3.2 Estimations of UV dose needed for 90%, 99%, and 99.9% airborne PRRSV reduction (Obj. 2)

Table 1 shows the parameters (including inactivation rate, *k*) of the one-stage and two-stage models derived from the experimental data.

Table 1. One-stage and two-stage models, parameter estimations, and model parameters for inactivation of airborne PRRSV with four types of UV light tested.

~~UV types~~	UV-C	UV-C	UV-A	UV-A

Preprints (www.preprints.org) | NOT PEER-REVIEWED | Posted: 2 March 2021 doi:10.20944/preprints202103.0068.v1

Parameters	(254 nm)	excimer (222 nm)	(365 nm, fluorescent)	(365 nm, LED)
Two-stage inactivation model				
Intercept	-0.0603	0.03226	0.012422	-0.02748
Susceptible virus population fraction (*f*)	0.97595	0.99945	0.57417	1.72542
Resistant virus population fraction (**1-*f***)	0.02405	0.00055	0.42583	-0.72542
Inactivation rate (constant), $\boldsymbol{k_1}$, for resistant virus population (cm^2/mJ)	-1.34467	-24.1466	-0.13585	0.88296
Inactivation rate (constant), $\boldsymbol{k_2}$, for susceptible virus population (cm^2/mJ)	15.55614	42.39715	2.89537	0.02075
Lack-of-fit test *p*-value	$p = 0.228$	$p = 0.8922$	$p = 0.2848$	$p = 0.6532$
One-stage inactivation model				
Intercept	-0.4727	-0.06694	-0.09103	0.08388
Inactivation rate, $\boldsymbol{k}$	4.8512	33.2674	0.01556	-0.02183
Lack-of-fit test *p*-value	$p = 0.006781$	$p = 0.1813$	$p = 0.3336$	$p = 0.7748$

Both inactivation curves of UV-C germicidal (254 nm) and UV-C excimer (222 nm) fit better (with lack-of-fit p-value >0.1) with a two-stage inactivation model rather than a one-stage inactivation model, with lack-of-fit p-value = 0.228 and 0.892, respectively. This finding is consistent with previous research on airborne PRRSV [21].

After incorporating the parameters from Table 1 to Eqn. (3) and (5), the model equations for each type of UV are expressed as follows.

For UV-C (254 nm) (data shown in Figure 2), one-stage and two-stage, respectively,

$$log_{10}\frac{N_t}{N_0} = -4.8512 \cdot D_t - 0.4727 \tag{6}$$

$$log_{10}\frac{N_t}{N_0} = log_{10}[0.02405 \cdot 10^{1.34467 \cdot D_t} + 0.97595 \cdot 10^{-15.55614 \cdot D_t}] - 0.0603 \tag{7}$$

For UV-C (222 nm) (data shown in Figure 3), one-stage and two-stage, respectively,

$$log_{10}\frac{N_t}{N_0} = -33.2674 \cdot D_t - 0.06694 \tag{8}$$

$$log_{10}\frac{N_t}{N_0} = log_{10}[0.00055 \cdot 10^{24.1466 \cdot D_t} + 0.99945 \cdot 10^{-42.39715 \cdot D_t}] + 0.03226 \tag{9}$$

For UV-A (365 nm, fluorescent) (data shown in Figure 4), one-stage and two-stage, respectively,

$$log_{10}\frac{N_t}{N_0} = -0.01556 \cdot D_t - 0.09103 \tag{10}$$

$$log_{10}\frac{N_t}{N_0} = log_{10}[0.42583 \cdot 10^{0.13585 \cdot D_t} + 0.57417 \cdot 10^{-2.89537 \cdot D_t}] + 0.012422 \tag{11}$$

For UV-C (365 nm, LED) (data shown in Figure 5), one-stage and two-stage, respectively,

$$log_{10}\frac{N_t}{N_0} = 0.02183 D_t + 0.08388 \tag{12}$$

$$log_{10}\frac{N_t}{N_0} = log_{10}[-0.72542 \cdot 10^{-0.88296 \cdot D_t} + 1.72542 \cdot 10^{-0.02075 \cdot D_t}] - 0.02748 \tag{13}$$

Table 2 summarized the estimated or projected UV doses for target percentage (%) PRRSV reduction of 90%, 99%, and 99.9%, based on one-stage and two-stage models.

Preprints (www.preprints.org) | NOT PEER-REVIEWED | Posted: 2 March 2021 doi:10.20944/preprints202103.0068.v1

Table 2. Estimated the UV dose (mJ/cm^2) needed for target % aerosolized PRRSV reduction in fast-moving air, using both one-stage and two-stage inactivation models.

	90% (1-log) reduction		99% (2-log) reduction		99.9% (3-log) reduction	
	1-stage	2-stage	1-stage	2-stage	1-stage	2-stage
UV-C (254 nm)	0.109	0.0681	0.315	0.0872	0.521[a]	0.0943
UV-C (222 nm)	0.0280	0.0246	0.0581	0.0429	0.0882	0.0483
UV-A (365 nm, fluor.)	58.42	-	122.684	-	186.952	-
UV-A (365 nm, LED)	-49.651[b]	58.285	-95.460[b]	106.478	-141.268[b]	154.671

[a] UV-C (254 nm) dose needed to inactivate 99.9% aerosolized PRRSV was estimated to be 1.21 mJ/cm^2 by Cutler et al. 2012 [20].
[b] Negative values are not considered biologically meaningful, i.e., the UV light under these categories did not have an inactivation effect for the doses used in the experiment.

3.3. Preliminary techno-economic analysis of potential farm-scale application (Obj. 3)

Table 3 shows the comparison of electricity cost (operational cost) among four different UV light types used for this laboratory-scale experiment.

Table 3. Comparison of electricity cost (operational cost) among four different UV light types used for this laboratory-scale experiment.

UV light	Measured power consumption (W) [a]	Electricity consumption (kWh)	Electricity cost [c]	Cost of UV lamps [d]
UV-C (254 nm)	50.5	0.038	$0.0023	< $100
UV-C (222 nm)	250	0.19	$0.0122	~ $600
UV-A (365 nm, fluor.)	49.5	0.037	$0.0022	< $100
UV-A (365 nm, LED)	43.8	0.033	$0.0019	~ $200 [e]

[a] The total power consumption of all lamps used for each experiment, i.e., 4 bulbs for UV-C (254 nm) and UV-A (fluorescent), respectively; 1 lamp for UV-C excimer, and 1 lamp for UV-A (LED); [b] The percentage of effective UV irradiated area (on PRRSV) with respect to its total irradiation area (estimated); [c] Electricity cost in rural areas (US Midwest) = $0.12/kWh; [d] Cost of UV lamps and fixtures, excluding other experimental devices, as described in the Material and Methods section; [e] Cost estimation of a research-grade prototype of the LED lamp (LED board + power supply).

Table 4 is a summary of preliminary cost estimation of UV application vs. HEPA filtration system.

Table 4. Estimations of the cost of implementing UV light or HEPA filtration treatment in a 1000-head swine barn with different swine types for 1 year. Estimations were based on extrapolations from this Laboratory-scale study.

Type	Capital cost (hot weather [a])	1-year electricity cost (mixed weather [a])	Maintainance	Total cost
UV light with pre-filters	$66,000	$35,000	$6,600	$107,600
HEPA filters with pre-filters	$80,400	N/A	$8,040	$ 88,440

[a] Estimations and assumptions on the size of the farm, ventilation rates, and weather conditions are from MWPS-8 "Swine Housing and Equipment Handbook" [39].

4. Discussion

4.1. UV effectiveness and inactivation models

Preprints (www.preprints.org) | NOT PEER-REVIEWED | Posted: 2 March 2021 doi:10.20944/preprints202103.0068.v1

To date, most of the research on ultraviolet inactivation of pathogens has been under static conditions, i.e., no viral aerosol generation or flow under UV irradiation. Only a fraction of such research involved dynamic targets, i.e., fast-moving aerosols rather than stationary cell plates or Petri dishes. There are much more UV irradiation experiments on stationary (static) objects than on dynamic (flowing) targets, so is the case for PRRSV treatment. Prior to the current research, Cutler et al. (2012) [20] was the benchmark on UV irradiation on aerosolized PRRSV. Other research experiments focused on stationary objects to inactivate PRRSV, e.g., on tissue culture plates [21], on common farm surfaces (rubber, concrete, paper, etc.) [40], on samples inside irradiation chamber [41].

In most cases, the UV doses cumulated in static systems were much higher than in dynamic systems because aerosols' flow significantly reduces the irradiation (contact) time on the targets (bacteria, viruses, etc.). However, according to Kowalski et al. (2000) [37], the UV inactivation rates tend to be higher in dynamic conditions than in static conditions, and thus less dose is needed. It was speculated that microbes flowing and tumbling in the air can receive UV irradiation all around, while under static conditions, the exposure is only directed in one plane or side, and thus it is less efficient.

The theoretical minimum titer determined using the Spearman-Kärber method was $1 \times 10^{0.5}$ (or 0.5 $\log_{10}$) $TCID_{50}$/mL. In this experiment, the detected PRRSV titer values were all above $1 \times 10^{1.5}$ $TCID_{50}$/mL, and the control samples (from Treatment 5) had a virus titer of about ~1×10^{4} $TCID_{50}$/mL. This research showed that the UV chamber achieve up to ~2-log reduction in aerosolized PRRSV with a UV dose < 0.3 mJ/cm^2 (UV-C, 254 nm), or < 0.08 mJ/cm^2 (UV-C, 222 nm), under experimental conditions. The experiment itself did not achieve a higher level of PRRSV titer reduction. Considering this, the estimation of 1-log and 2-log airborne PRRSV reductions was reasonable and within the data scope, while estimation for 3-log reduction would be less accurate than the former two. Thus, the model was extrapolated to estimate the dose needed for a higher reduction level (i.e., >2-log). The model's accuracy could be improved if the data represent a wider range of UV doses inactivating higher PRRSV titers. To estimate a UV dose required for a higher log reduction would require a higher initial concentration of virus load to start with. Extending the sampling time may increase the initial PRRSV titer, but a very long sampling time may reduce virus viability before titration and thus reduce the virus titer's accuracy derived from cell culture plates.

The experimental data were evaluated using both one-stage and two-stage fit with inactivation models for all four types of UV light used in this experiment. The two-stage model provided a better fit with both UV-C 254 nm and UV-C 222 nm, with lack-of-fit *p*-values of 0.228 and 0.892 (both >0.1), respectively. Due to the magnitude difference of doses needed for 3-log reduction between one-stage and two-stage models, 0.521 and 0.0943 mJ/cm^2, respectively, we reported both values for consideration, but 0.521 mJ/cm^2 is more realistic and similar to the dose 1.21 mJ/cm^2 reported by Cutler et al. (2012) [20]. The estimated UV-C (222 nm) doses were similar between one-stage and two-stage models.

For UV-A (365 nm) (both fluorescent and LED-based), the reduction of PRRSV titer was not found for the dose up to 4.11 mJ/cm^2. This experiment does not rule out UV-A's effectiveness, but a much higher UV dose may be needed to achieve the same log reduction or to have a significant germicidal effect.

4.2. Exploring the UV inactivation mechanism

UV light inactivates pathogens by causing the DNA or RNA structure to distort, and thus a normal replication cannot happen. However, it does not directly "kill" the pathogen (bacteria or viruses); at least, this is not its primary means of inactivation, although, at a higher dose, this may happen by speculation. Thus, to understand and verify the mechanism of UV irradiation on PRRSV, an additional PCR test could be added in this experiment. If the PCR results show no significant reduction while bioassay does, that could help confirm the mechanism of UV inactivation.

4.3. Techno-economic analysis

Per feasibility evaluation, due to the high cost of UV-C excimer (in the magnitude of thousand USD per lamp), the economic analysis was only conducted for UV-C (254 nm) lamp to consider its feasibility for farm-scale application. Cost comparison for a 1,000-head swine barn, 1-y maintenance was conducted between the UV light and HEPA filtration systems. The estimation indicated that UV-C light cost is estimated to be $107,600 while HEPA filtration costs approximately $88,400. The cost difference is within 25%. However, UV lamps usually need to be replaced after 8,000 h (<1-y) of operation, while HEPA filters typically last for a few years if maintained well. On the other hand, the UV light system is less labor-intensive for monitoring and replacements. The UV light can be turned off when the risk is low, thus allowing farmers to make cost-conscious decisions. Based on these two factors, the cost comparison for a long-term implementation deserves more data collection and study to lead to a more data-driven metric.

5. Conclusions

The results show that UV-C (254 nm) and UV-C excimer (222 nm) effectively inactivated aerosolized PRRSV up to 99% (2-log) with a dose <0.3 mJ/cm^2 for UV-C (254 nm) dose, or <0.08 mJ/cm^2 for UV-C (222 nm). UV doses needed for 1-log, 2-log, and 3-log virus titer reductions were estimated using both one-stage and two-stage inactivation models. For both types of UV-A (365 nm) lamps, no reduction of PRRSV titer was found with the UV dose used in this experiment. This experiment does not rule out UV-A effectiveness, but a much higher UV dose may be needed. Preliminary economic analysis showed that UV light costs the same magnitude as HEPA filtration systems in terms of materials and electricity at a farm-scale implementation. However, more data and research are needed to make accurate and long-term predictions.

Supplementary Materials: The following are available online at www.mdpi.com/xxx/. Supplementary Figures S1 – S5 show the UV lamps used in this experiment, as well as demonstrations of measuring light intensity. A well-organized Excel spreadsheet (UV dose vs. PRRSV titer.xlsx) is provided, including UV doses and infectious PRRSV titer data.

Author Contributions: Conceptualization, JK, JJZ, SH, WJ; methodology, JK, JJZ, JZ, PL, TC, WY; validation, PL, JK, JJZ, TC, ML, BC; formal analysis, PL, TC; investigation PL, TC; resources PL, JK, TC, WY, JJZ, JZ; data curation PL, TC; writing – original draft preparation, PL; writing – review and editing, JK, JJZ, JZ, WJ, PL; visualization, PL; supervision, JK, JJZ, JZ; project administration, JK, JJZ; funding acquisition, JK, JJZ, JZ, WJ, SH. All authors have read and agreed to the published version of the manuscript.

Funding: This project was funded by checkoff dollars through the National Pork Board (NPB). (Project Title: Mitigation of PRRS transmission with UV light treatment of barn inlet air: proof-of-concept. Project number: NPB #18-160. In addition, this research was partially supported by the Iowa Agriculture and Home Economics Experiment Station, Ames, Iowa. Project no. IOW05556 (Future Challenges in Animal Production Systems: Seeking Solutions through Focused Facilitation) sponsored by the Hatch Act and State of Iowa funds (JK).

Institutional Review Board Statement: The Institutional Biosafety Committee (IBC) of Iowa State University approved the study on April 14, 2020. Protocol code: IBC-20-016. Title: Mitigation of PRRS transmission with UV light treatment of barn inlet air: proof-of-concept.

Data Availability Statement: The raw data is available in a spreadsheet (UV dose vs. PRRSV titer.xlsx), which is accessible at xxx.

Acknowledgments: The authors are very thankful to Haiyan Huang (Veterinary Diagnostic Laboratory staff) for her help on lab skill improvements, Dr. Chumki Banik for her help with purchasing, Danielle Wrzesinski for her help in preparing the experimental setup, Dr. Aaron Stephan and Hoa-Thanh Huynh from ONCE Inc. for the research prototype LED lamp.

Conflicts of Interest: The authors declare no conflict of interest. The funders had no role in the design of the study, in the collection, analyses, or interpretation of data, in the writing of the manuscript, or in the decision to publish the results.

Appendix A

Preprints (www.preprints.org) | NOT PEER-REVIEWED | Posted: 2 March 2021 doi:10.20944/preprints202103.0068.v1

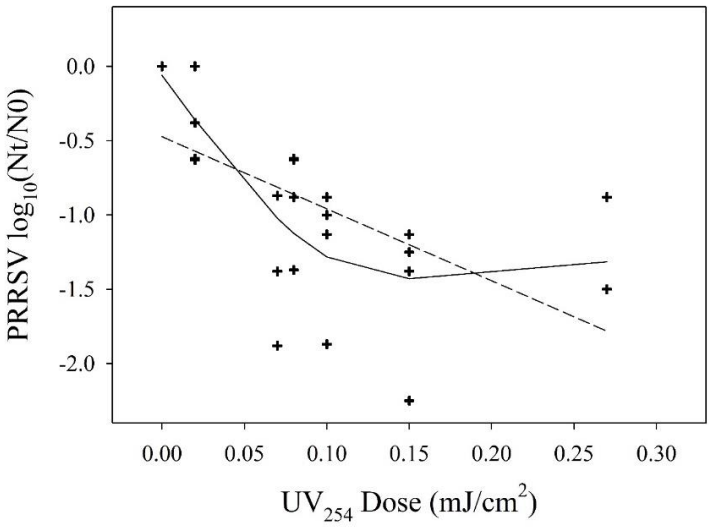

Figure A1. UV-A (254 nm) treatment inactivation curve on aerosolized PRRSV. One-stage (dashed line) and two-stage (solid line) inactivation curves were drawn. PRRSV survival is expressed as $\log_{10}(N_t/N_0)$, not as a percentage (%) as shown in Figure 2.

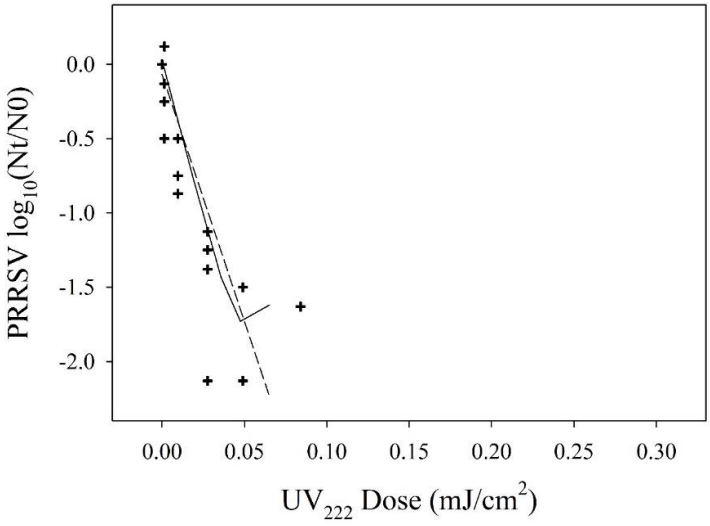

Figure A2. UV-C (222 nm) treatment inactivation curve on aerosolized PRRSV. One-stage (dashed line) and two-stage (solid line) inactivation curves were drawn. PRRSV survival is expressed as $\log_{10}(N_t/N_0)$, not as a percentage (%) as shown in Figure 3.

Preprints (www.preprints.org) | NOT PEER-REVIEWED | Posted: 2 March 2021 doi:10.20944/preprints202103.0068.v1

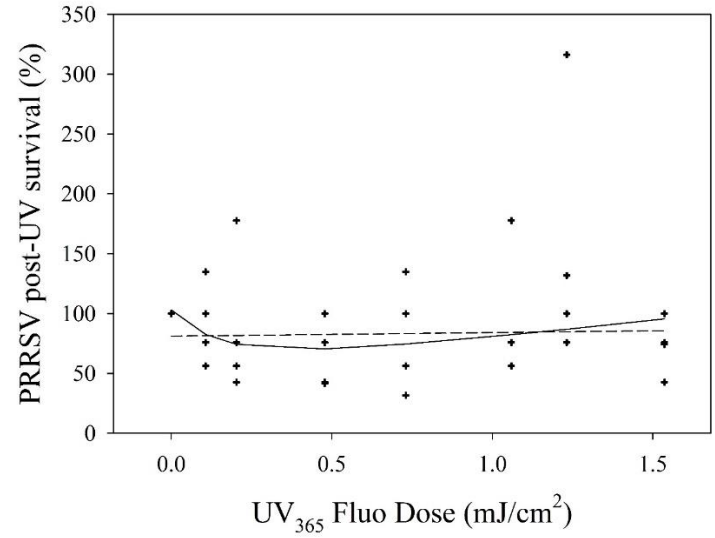

Figure A3. UV-A (365 nm, fluorescent) treatment inactivation curve on aerosolized PRRSV. One-stage (dashed line) and two-stage (solid line) inactivation curves were drawn. PRRSV survival is expressed as $\log_{10}(N_t/N_0)$, not as a percentage (%) as shown in Figure 4.

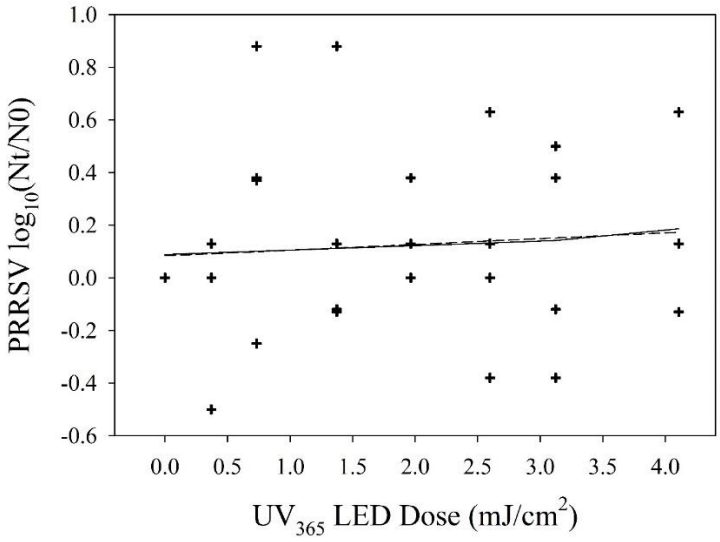

Figure A4. UV-A (365 nm, LED) treatment inactivation curve on aerosolized PRRSV. One-stage (dashed line) and two-stage (solid line) inactivation curves were drawn. PRRSV survival is expressed as $\log_{10}(N_t/N_0)$, not as a percentage (%) shown in Figure 5.

Preprints (www.preprints.org) | NOT PEER-REVIEWED | Posted: 2 March 2021 doi:10.20944/preprints202103.0068.v1

Appendix B

Treatment 1	0.09	0.12	0.12	0.13	0.13	0.11	0.09
Treatment 2	0.09	0.14	0.15	0.16	0.16	0.14	0.11
Treatment 3	0.10	0.15	0.16	0.18	0.18	0.15	0.12
Treatment 4	0.11	0.17	0.18	0.19	0.19	0.16	0.12
Treatment 5	0.10	0.16	0.17	0.19	0.19	0.17	0.13
Treatment 6	0.11	0.15	0.17	0.18	0.18	0.16	0.12
Treatment 7	0.09	0.14	0.14	0.15	0.15	0.14	0.10
Treatment 8	0.07	0.11	0.12	0.12	0.12	0.10	0.08

Figure B1. Map UV light intensity (irradiance) measurements for UV-C (254 nm) for Treatment 1 to Treatment 8. Each colored grid represents a ~ 4 x 4 cm area (point) where the UV sensor was in place for measurement. The color gradient green-yellow-red represents increasing UV light intensity. Units: mW/cm^2.

Treatment 1	0.022	0.030	0.038	0.040	0.030	0.021	0.015
Treatment 2	0.027	0.045	0.056	0.056	0.044	0.027	0.020
Treatment 3	0.030	0.046	0.058	0.058	0.047	0.027	0.020
Treatment 4	0.035	0.047	0.060	0.061	0.049	0.030	0.022
Treatment 5	0.032	0.046	0.060	0.060	0.047	0.030	0.022
Treatment 6	0.032	0.048	0.061	0.060	0.049	0.031	0.021
Treatment 7	0.033	0.047	0.060	0.059	0.047	0.031	0.021
Treatment 8	0.029	0.044	0.057	0.055	0.043	0.029	0.018

Figure B2. Map UV light intensity (irradiance) measurements for UV-C (222 nm) for Treatment 1 to Treatment 8. The color gradient green-yellow-red represents increasing UV light intensity. Units: mW/cm^2.

Preprints (www.preprints.org) | NOT PEER-REVIEWED | Posted: 2 March 2021 doi:10.20944/preprints202103.0068.v1

Treatment 1	0.42	0.55	0.64	0.67	0.66	0.61	0.45
Treatment 2	0.49	0.73	0.80	0.80	0.78	0.75	0.57
Treatment 3	0.54	0.81	0.86	0.87	0.88	0.82	0.63
Treatment 4	0.54	0.84	0.90	0.91	0.92	0.84	0.64
Treatment 5	0.50	0.83	0.89	0.90	0.91	0.85	0.65
Treatment 6	0.47	0.77	0.84	0.84	0.85	0.81	0.63
Treatment 7	0.42	0.69	0.75	0.74	0.76	0.71	0.56
Treatment 8	0.29	0.50	0.60	0.59	0.55	0.49	0.39

Figure B3. Map UV light intensity (irradiance) measurements for UV-A (365 nm, fluorescent) for Treatment 1 to Treatment 8. The color gradient green-yellow-red represents increasing UV light intensity. Units: mW/cm^2.

Treatment 1	1.44	1.60	1.89	1.96	1.91	1.70	1.50
Treatment 2	1.51	1.91	2.08	2.12	2.09	2.01	1.81
Treatment 3	1.51	1.96	2.16	2.21	2.20	2.07	1.87
Treatment 4	1.47	1.93	2.18	2.24	2.25	2.12	1.91
Treatment 5	1.45	1.92	2.16	2.23	2.24	2.15	1.90
Treatment 6	1.50	1.92	2.13	2.20	2.22	2.13	1.83
Treatment 7	1.42	1.86	2.04	2.09	2.12	2.03	1.72
Treatment 8	1.19	1.65	1.87	1.88	1.79	1.70	1.52

Figure B4. Map UV light intensity (irradiance) measurements for UV-C (365 nm, LED) for Treatment 1 to Treatment 8. The color gradient green-yellow-red represents increasing UV light intensity. Units: mW/cm^2.

Figure B5. The layout of UV irradiation for all eight treatments. Each treatment represents a quartz tube, which is equally "divided" into seven sections. The colored grid indicates areas of UV irradiations while blank spaces are shielded from UV with sections of PVC tubes over the quartz tubes. The arrangement of the layout is randomly selected and remained the same for the experiments.

References

1. Terpstra, C.; Wensvoort, G.; Pol, J.M.A. Experimental reproduction of PEARS (mystery swine disease) by infection with Lelystad virus: Koch's postulates fulfilled. *Veterinary Quarterly* **1991**, *13*, 131–136.
2. Wensvoort, G.; Terpstra, C.; Pol, J.M.A.; ter Laak, E. A.; Bloemraad, M.; de Kluyver, E.P.; Kragten, C.; van Buiten, L.; den Besten, A.; Wagenaar, F.; Broekhuijsen, J.M.; Moonen, P.L.J.M.; Zetstra, T.; de Boer, E.A.; Tibben, H.J.; de Jong, M.F.; van 't Veld, P.; Greenland, G.J.R.; van Gennep, J.A.; Voets, M.T.; Verheijden, J.H.M.; Braamskamp, J. Mystery swine disease in the Netherlands: The isolation of Lelystad virus. *Veterinary Quarterly* **1991**, *13*, 121–130. doi: 10.1080/01652176.1991.9694296.
3. Neumann, E.J.; Kliebenstein, J.B.; Johnson, C.D.; Mabry, J.W.; Bush, E.J.; Seitzinger, A.H.; Green, A.L.; Zimmerman, J.J. Assessment of the economic impact of porcine reproductive and respiratory syndrome on swine production in the United States. *Journal of the American Veterinary Medical Association* **2005**, *227*, 385–392. doi: 10.2460/javma.2005.227.385.
4. Holtkamp, D. J.; Kliebenstein, J. B.; Zimmerman, J. J.; Neumann, E., Rotto, H., Yoder, T. K., et al. (2013). Assessment of the Economic Impact of Porcine Reproductive and Respiratory Syndrome Virus on US Pork Producers. Assessment of the Economic Impact of Porcine Reproductive and Respiratory Syndrome Virus on US Pork Producers. *J Swine Heal Prod* **2013**, 21, 72–84. doi:10.31274/ans_air-180814-28.
5. Miller, M. *Pork Checkoff Report*. June 2017, pp. 38–39.
6. Nathues, H.; Alarcon, P.; Rushton, J.; Jolie, R.; Fiebig, K.; Jimenez, M.; Geurts, V.; Nathues, C. Cost of porcine reproductive and respiratory syndrome virus at individual farm level – An economic disease model. *Preventive Veterinary Medicine* **2017**, *142*, 16–29.
7. Lager, K.M.; Mengeling, W.L. American Association of Swine Practitioners 2000 Annual Meeting. In Experimental aerosol transmission of pseudorabies virus and porcine reproductive and respiratory syndrome virus; AASP: Indianapolis, Indiana, 2000; pp. 409–410.
8. Otake, S.; Dee, S.A.; Jacobson, L.; Pijoan, C.; Torremorell, M. Evaluation of aerosol transmission of porcine reproductive and respiratory syndrome virus under controlled field conditions. *Veterinary Record* **2002**, *150*, 804–808. doi:10.1136/vr.150.26.804.
9. Torremorell, M.; Pijoan, C.; Janni, K.; Walker, R.; Joo, H.S. Airborne transmission of Actinobacillus pleuropneumoniae and porcine reproductive and respiratory syndrome virus in nursery pigs. *American Journal of Veterinary Research* **1997**, *58*, 828–832.
10. Wills, R.W.; Zimmerman, J.J.; Swenson, S.L.; Yoon, K.J.; Hill, H.T.; Bundy, D.S.; McGinley, M.J. Transmission of PRRSV by direct, close, or indirect contact. *Journal of Swine Health and Production* **1997**, *5*, 213–218.
11. Dee, S.; Otake, S.; Oliveira, S.; Deen, J. Evidence of long distance airborne transport of porcine reproductive and respiratory syndrome virus and Mycoplasma hyopneumoniae. *Veterinary Research* **2009**, *40*, 39.
12. Otake, S.; Dee, S.; Corzo, C.; Oliveira, S.; Deen, J. Long-distance airborne transport of infectious PRRSV and Mycoplasma hyopneumoniae from a swine population infected with multiple viral variants. *Veterinary Microbiology* **2010**, *145*, 198–208. doi: 10.1016/j.vetmic.2010.03.028.
13. La, A.; Zhang, Q.; Levin, D.B.; Coombs, K.M. The Effectiveness of Air Ionization in Reducing Bioaerosols and Airborne PRRS Virus in a Ventilated Space. *Transactions of the ASABE* **2019**, *62*, 5, 1299-1314. doi: 10.13031/trans.13430.
14. Xia, T.; Lin, Z.; Lee, E.M.; Melotti, K.; Rohde, M.; Clack, H.L. Field Operations of a Pilot Scale Packed-bed Non-thermal Plasma (NTP) Reactor Installed at a Pig Barn on a Michigan Farm to Inactivate Airborne Viruses. In 2019 IEEE Industry Applications Society Annual Meeting (pp. 1-4). IEEE.

15. Dee, S.; Otake, S.; Deen, J. An evaluation of ultraviolet light (UV254) as a means to inactivate porcine reproductive and respiratory syndrome virus on common farm surfaces and materials. *Veterinary Microbiology* **2011**, *150*, 96–99. doi: 10.1016/j.vetmic.2011.01.014.
16. Nan, Y.; Wu, C.; Gu, G.; Sun, W.; Zhang, Y.-J.; Zhou, E.-M. Improved Vaccine against PRRSV: Current Progress and Future Perspective. *Frontiers in Microbiology* **2017**, *8*. doi: 10.3389/fmicb.2017.01635
17. Dee, S.; Joo, H. Prevention of the spread of porcine reproductive and respiratory syndrome virus in endemically infected pig herds by nursery depopulation. *Veterinary Record* **1994**, *135*, 6–9.
18. Dee, S.; Batista, L.; Deen, J.; Pijoan, C. Evaluation of an air-filtration system for preventing aerosol transmission of porcine reproductive and respiratory syndrome virus. *Can. J. Vet. Res*. **2005**, 69, 293–298.
19. Dee, S., Otake, S., and Deen, J. Use of a production region model to assess the efficacy of various air filtration systems for preventing airborne transmission of porcine reproductive and respiratory syndrome virus and Mycoplasma hyopneumoniae: Results from a 2-year study. *Virus Research* **2010**, *154*, 177–184. doi: 10.1016/j.virusres.2010.07.022.
20. Cutler, T.D.; Wang, C.; Hoff, S.J., Zimmerman, J.J. Effect of temperature and relative humidity on ultraviolet (UV254) inactivation of airborne porcine respiratory and reproductive syndrome virus. *Veterinary Microbiology*, **2012**, *159*, 47–52. doi: 10.1016/j.vetmic.2012.03.044.
21. Cutler, T.; Wang, C.; Qin, Q.; Zhou, F.; Warren, K.; Yoon, K.-J.; Hoff, S. J.; Ridpath, J.; Zimmerman, J. Kinetics of UV254 inactivation of selected viral pathogens in a static system. *Journal of Applied Microbiology* **2011**, *111*, 389–395.
22. Buonanno, M.; Ponnaiya, B.; Welch, D.; Stanislauskas, M.; Randers-Pehrson, G.; Smilenov, L.; Lowy, F. D.; Owens, D. M.; Brenner, D. J. Germicidal Efficacy and Mammalian Skin Safety of 222-nm UV Light. *Radiation Research* **2017**, *187*, 493–501.
23. Welch, D.; Buonanno, M.; Grilj, V.; Shuryak, I.; Crickmore, C.; Bigelow, A.W.; Randers-Pehrson, G.; Johnson, G. W.; Brenner, D. J. Far-UVC light: A new tool to control the spread of airborne-mediated microbial diseases. *Scientific Reports* **2018**, *8*, 2752. doi: 10.1038/s41598-018-21058-w.
24. Yang, X.; Koziel, J.A.; Laor, Y.; Zhu, W.; van Leeuwen, J.; Jenks, W.S.; Hoff, S.J.; Zimmerman, J.; Zhang, S.; Ravid, U.; Armon, R. VOC Removal from Manure Gaseous Emissions with UV Photolysis and UV-TiO2 Photocatalysis. *Catalysts* **2020**, *10*, 607. doi: 10.3390/catal10060607.
25. Lee, M.; Koziel, J.A.; Murphy, W.; Jenks, W.S.; Fonken, B.; Storjohann, R.; Chen, B.; Li, P.; Banik, C.; Wahe, L.; Ahn, H. Design and Testing of Mobile Laboratory for Mitigation of Gaseous Emissions from Livestock Agriculture with Photocatalysis. *Int. J. Environ. Res. Public Health* **2021**, 18, 1523. doi: 10.3390/ijerph18041523.
26. Lee, M.; Li, P.; Koziel, J.A.; Ahn, H.; Wi, J.; Chen, B.; Meiirkhanuly, Z.; Banik, C.; Jenks, W.S. Pilot-Scale Testing of UV-A Light Treatment for Mitigation of NH3, H2S, GHGs, VOCs, Odor, and O3 Inside the Poultry Barn. *Frontiers in Chemistry* **2020**, *8*, 613; doi: 10.3389/fchem.2020.00613.
27. Lee, M.; Wi, J.; Koziel, J.A.; Ahn, H.; Li, P.; Chen, B.; Meiirkhanuly, Z.; Banik, C.; Jenks, W. Effects of UV-A Light Treatment on Ammonia, Hydrogen Sulfide, Greenhouse Gases, and Ozone in Simulated Poultry Barn Conditions. *Atmosphere* **2020**, *11*, 283. doi: 10.3390/atmos11030283.
28. Maurer, D.; Koziel, J.A. On-farm pilot-scale testing of black ultraviolet light and photocatalytic coating for mitigation of odor, odorous VOCs, and greenhouse gases. *Chemosphere*, **2019**, *221*, 778-784; doi: 10.1016/j.chemosphere.2019.01.086.
29. Zhu, W.; Koziel, J.A.; Maurer, D.L. Mitigation of Livestock Odors Using Black Light and a New Titanium Dioxide-Based Catalyst: Proof-of-Concept. *Atmosphere* **2017**, *8*, 103. doi: 10.3390/atmos8060103.
30. Li, P.; Koziel, J.A.; Zimmerman, J.; Hoff, S.; Zhang, J.; Cheng, T.; Yim-Im, W.; Lee, M.; Chen, B.; Jenks, W. Designing and Testing of a System for Aerosolization and Recovery of Viable Porcine Reproductive and Respiratory Syndrome Virus (PRRSV): Theoretical and Engineering Considerations. *Preprints* 2021. doi: 10.20944/preprints202102.0253.v1.
31. Koziel, J.A., Zimmerman, J.J., Jenks, W.S., Hoff, S. Mitigation of PRRS transmission with UV light treatment of barn inlet air: proof-of-concept. National Pork Board, Des Moines, IA; Project 18-160. Final Report, Dec 2020.
32. Kim, H.S.; Kwang, J.; Yoon, I.J.; Joo, H.S.; Frey, M.L. Enhanced replication of porcine reproductive and respiratory syndrome (PRRS) virus in a homogeneous subpopulation of MA-104 cell line. *Archives of Virology* **1993**, *133*, 477–483.
33. Hermann, J.R.; Hoff, S.J.; Yoon, K.J.; Burkhardt, A.C.; Evans, R.B.; Zimmerman, J.J. Optimization of a Sampling System for Recovery and Detection of Airborne Porcine Reproductive and Respiratory Syndrome Virus and Swine Influenza Virus. *Applied and Environmental Microbiology* **2006**, *72*, 4811–4818. doi:10.1128/aem.00472-06.
34. Hamilton, M.A.; Russo, R.C.; Thurston, R. V. Trimmed Spearman-Karber method for estimating median lethal concentrations in toxicity bioassays. *Environmental Science & Technology* **1977**, *11*, 714–719.
35. Cecil, H.R.J. In *Techniques in experimental virology*; Academic Press, **1964**; pp. 183–186.
36. Karber, G. Beitrag zur kollektiven Behandlung pharmakologischer Reihenversuche. *Arch Exp. Path. Pharmakol* **1931**, *162*, 480–483.
37. Kowalski, W.J.; Bahnfleth, W.P.; Witham, D.L.; Severin, B.F.; Whittam, T.S. *Quantitative Microbiology* **2000**, *2*, 249–270.
38. Riley, R.L.; Kaufman, J.E. Effect of Relative Humidity on the Inactivation of Airborne Serratia marcescens by Ultraviolet Radiation. *Appl Microbiol.* **1972**, *23*, 1113–1120.
39. *MWPS-8 Swine Housing and Equipment Handbook*; 4th ed.; Iowa State University: Ames, IA, 1983.
40. Dee, S.; Otake, S.; Deen, J. An evaluation of ultraviolet light (UV254) as a means to inactivate porcine reproductive and respiratory syndrome virus on common farm surfaces and materials. *Veterinary Microbiology* **2011**, *150*, 96–99.
41. Stephan, A. B. Reduction in swine pathogen numbers by a UVC germicidal chamber https://www.nationalhogfarmer.com/animal-health/reduction-swine-pathogen-numbers-uvc-germicidal-chamber (accessed 9 February 2021).